



Published in final edited form as:

Stem Cells. 2011 February ; 29(2): . doi:10.1002/stem.584.

Transplanted stem cell-secreted VEGF effects post-stroke recovery, inflammation, and vascular repair

Nobutaka Horie^{*}, Marta P. Pereira^{*}, Kuniyasu Niizuma, Guohua Sun, Hadar Keren-Gill, Angelo Encarnacion, Mehrdad Shamloo, Scott A. Hamilton, Kewen Jiang, Stephen Huhn¹, Theo D. Palmer, Tonya M. Bliss^{**}, and Gary K. Steinberg^{**}

Department of Neurosurgery and Stanford Stroke Center, Stanford Institute for Neuro-Innovation and Translational Neurosciences, Stanford University School of Medicine, Stanford, California, USA

¹StemCells Inc, Palo Alto, California, USA

Abstract

Cell transplantation offers a novel therapeutic strategy for stroke; however, how transplanted cells function in vivo is poorly understood. We show for the first time that after sub-acute transplantation into the ischemic brain of human central nervous system stem cells grown as neurospheres (hCNS-SCns), the stem cell-secreted factor, human VEGF (hVEGF), is necessary for cell-induced functional recovery. We correlate this functional recovery to hVEGF-induced effects on the host brain including multiple facets of vascular repair, and its unexpected suppression of the inflammatory response. We found that transplanted hCNS-SCns affected multiple parameters in the brain with different kinetics: early improvement in blood-brain barrier (BBB) integrity and suppression of inflammation was followed by a delayed spatio-temporal regulated increase in neovascularization. These events coincided with a bi-modal pattern of functional recovery: an early recovery independent of neovascularization, and a delayed hVEGF-dependent recovery coincident with neovascularization. Therefore, cell transplantation therapy

Correspondence and requests for reprints to: Tonya Bliss, PhD, tbliss1@stanford.edu, Dept Neurosurgery, 1201 Welch Rd, Stanford, CA 94305-5487, USA, Tel: +1 650 723 2004, Fax: +1 650 736 1949 or Gary K. Steinberg, MD, PhD, gsteinberg@stanford.edu, Dept Neurosurgery, 1201 Welch Rd, Stanford, CA 94305-5487, USA, Tel: +1 650 725 5562, Fax: +1 650 723 2815.

^{*}These authors contributed equally to this work

^{**}Co-senior authors

Nobutaka Horie has moved to the Department of Neurosurgery, Nagasaki University School of Medicine, 1-7-1, Sakamoto, Nagasaki, Japan, 852-8501

Disclosure of Potential Conflicts of Interest:

S.H. is a full time employee of StemCells Inc, the company that provided the cells, and has equity (stock) in the company. The other authors have no financial interests to disclose.

Author Contributions:

Nobutaka Horie: Design, collection and assembly of data, data analysis and interpretation, manuscript writing

Kuniyasu Niizuma: Collection and assembly of data, data analysis and interpretation

Marta P. Pereira: Design, collection and assembly of data, data analysis and interpretation, manuscript writing

Guohua Sun: Collection of data

Hadar Keren-Gill: Collection of data

Angelo Encarnacion: Collection of data

Mehrdad Shamloo: Collection of data

Scott A. Hamilton: Statistical analysis advice

Kewen Jiang: Collection of data

Stephen Huhn: Provision of study material, manuscript writing

Theo D. Palmer: Data analysis and interpretation

Tonya M. Bliss: Conception and design, data analysis and interpretation, manuscript writing, final approval of manuscript

Gary K. Steinberg: Financial support, design, data interpretation, manuscript writing, final approval of manuscript

offers an exciting multi-modal strategy for brain repair in stroke and potentially other disorders with a vascular or inflammatory component.

Keywords

angiogenesis; blood brain barrier; dystroglycan; inflammation; Avastin

INTRODUCTION

Stroke is a leading cause of long term disability with very few therapeutic options. Due to its complex pathology including damage to neurons, glia, and endothelial cells in the brain, conventional therapeutic strategies target the first few critical hours after stroke onset to minimize stroke-induced damage. Cell transplantation presents a novel therapeutic approach with the potential to repair the damaged brain and therefore extend the therapeutic time window of intervention, thus benefiting significantly more stroke patients. A diverse array of transplanted cell types, including brain-, bone marrow-, and blood-derived progenitors are reported to enhance functional recovery after stroke [1–6], and several cell transplantation clinical trials for stroke are currently underway [7]. The cells used in this study - human central nervous system stem cells grown as neurospheres or hCNS-SCns - are a potentially exciting candidate for stroke therapy as they are currently in clinical trials for several other CNS disorders (<http://www.stemcellsinc.com>).

Despite multiple reports indicating that stem cell transplantation is beneficial after stroke, the mechanisms of stem cell-induced recovery are poorly understood and may differ depending on the cell type studied. Secretion of trophic factors by transplanted cells is speculated to be a major contributor to their beneficial effects, but it is not known which factors are necessary to elicit recovery. Several studies have overexpressed factors in transplanted stem cells and found recovery was further enhanced [8, 9]; however, such experiments do not elucidate whether these factors are sufficient to stimulate recovery or whether they can only amplify recovery in an already primed system. Therefore, identification of crucial stem cell-secreted factors remains to be determined. Furthermore, it is not understood what changes occur in the brain in response to the grafted stem cells, the role of stem cell-secreted factors in these changes, or how they relate to stem cell-induced recovery; understanding such a cause and effect relationship will be imperative to understanding the mechanism of action of transplanted cells.

In this study we begin to address these questions by selectively neutralizing vascular endothelial growth factor (VEGF) secreted by transplanted hCNS-SCns and investigating how this affects functional recovery and various stem cell-induced changes in the post-stroke brain. We chose to study VEGF because it is a key pro-angiogenic factor and increased vascularization and perfusion in the peri-infarct region within a few days after stroke is associated with neurological recovery in patients [10, 11]. Moreover, acute transplantation of bone marrow- or blood-derived cells after stroke enhances blood vessel formation and, in some studies, functional recovery in rodents [12–14]. It is therefore postulated that stem cell-induced vascularization after stroke is important for cell-induced recovery [15, 16]. Additionally, the tight network of communication between the vasculature and the neurovascular unit, which is comprised of neurons, astrocytes and microglia [17], implies that effects on the vasculature have the potential to significantly influence brain function [16]. Inflammation, another major determinant of stroke pathology, can also affect vascularization and blood-brain barrier (BBB) integrity through release of pro-angiogenic factors and reactive oxygen species [18, 19], and there is growing evidence that interactions between the neurovascular unit and inflammation are also critical to stroke recovery [20].

Moreover, stem cell transplantation is reported to decrease inflammation in rodent models of stroke and multiple sclerosis [21–25], but it is not understood how.

In summary, this study investigates for the first time the *in vivo* role of a stem cell-secreted factor in mediating functional recovery in the stroke brain. We neutralize VEGF secreted by transplanted hCNS-SCNs, determine how this alters stem cell-induced functional recovery, and relate this to changes in stem cell-mediated effects on vascular regeneration including neovascularization, restoration of blood brain barrier (BBB) integrity, and neuroinflammation, which are all postulated to significantly influence post-stroke recovery.

MATERIALS and METHODS

Distal middle cerebral artery occlusion (dMCAo) and cell transplantation

Animal procedures were approved by Stanford University's Administrative Panel on Laboratory Animal Care. T cell-deficient adult male Nude rats [26] (Cr: NIH-RNU 230 ± 30 g) were subjected to permanent dMCAo with 0.5 h bilateral CCA occlusion as described [27] under isoflurane anesthesia. 1 mg/ml Ampicillin was administered daily orally 3 days before stroke surgery to 7 days post-transplantation surgery.

Fetal-derived hCNS-SCNs [28] were dissociated for transplantation [27]. Three 1.0 µl cell deposits (1×10^5 cells/µl) or vehicle were injected into the ipsilesional cortex at 7 days post-dMCAo as described [27]: (i) anterior–posterior (A–P), +1.6; medial–lateral (M–L), –2.4; dorsal–ventral (D–V), –2.4; (ii) A–P, +0.7; M–L, –2.4; D–V, –2.4; (iii) A–P, –0.3; M–L, –2.4; D–V, –2.4. For 'dead cell' transplants the cells went through four cycles of freeze thaw using dry ice and a waterbath, prior to transplantation.

Tissue Processing, measurement of cortical atrophy, and cell survival

Rats were perfused and 40 µm coronal sections prepared [27]. Cortical atrophy at 4 weeks post-transplantation was measured (blinded) in cresyl violet-stained sections by a semi-stereological approach. Animals were chosen at random from each group. Five serial sections, 0.5 mm apart starting at A–P +1.7, were taken per brain, as this encompassed the lesion. The remaining ipsilesional cortex was measured and divided by the area of the contralateral cortex. hCNS-SCNs survival in animals chosen randomly at 2 weeks post-transplantation was determined (blinded) by stereological counting as previously described [27].

Immunohistochemistry and inflammation analysis

Primary antibodies were incubated overnight, 4°C [27]: SC121 (1:500; human cytoplasmic marker, StemCells, Inc.), anti-dystroglycan (DG, 1:100, Novocastra), rabbit anti-aquaporin 4 (1:500, Sigma), anti-human VEGFa (1:100, Abcam), anti-Iba 1 (1:1000, Waco), Cy3 F(ab)2 Frag donkey anti-human IgG (1:500, Jackson), anti-β-tubulin (1:1000, Millipore), anti-nestin (1:250, Abcam), anti-human nuclei (1:100, Millipore). Secondary antibodies were incubated 2 h at room temperature (1:1000, Alexa Fluor 568 or 488, Jackson ImmunoResearch), with DAPI (1:1,000, Calbiochem), followed by confocal microscopy analysis. Cell lysates were measured for hVEGF by ELISA using the Quantikine human VEGF kit (R&D Systems).

Stereological quantification of IBA-1 stained microglia/monocytes was done as described [27]. Four sections/animal (each 40 µm apart spanning A–P 1.0 to 0.5 mm encompassing the majority of the lesion) were blindly analyzed using Stereo Investigator (MBF Bioscience) and average density determined. Two regions of interest (ROIs) were counted per slice, the peri-infarct region (defined in Figure 6A) and the remainder of the ipsilesional cortex. Two

sections/animal were counted for Avastin- and IgG-treated animals; this gave similar trends to counting 4 sections.

Blood vessel density analysis

Vessels were labeled by jugular vein injection of FITC-lectin (1.6 mg/kg, Vector) 30 min pre-sacrifice. Blood vessel density (BVD) was measured (blinded) using Image J to determine pixel number/image. The ratio of ipsi/contra BVD was calculated. BVD was analyzed in 3 ROIs: the cortical ischemic penumbra; near the graft; between the two, and in equivalent ROIs in the contralateral cortex. In each of the ROIs, 3 sub-ROIs were imaged to sample vessels from different cortical layers. Three sections were analyzed per animal in the same A-P region defined above. Thus, for each ROI, 9 images were analyzed per hemisphere and the average of these BVD ratios taken. Vessel width was also measured as it could affect pixel number. There was no significant difference in average vessel width in the absence of antibody treatment. Animals receiving intraperitoneal injections had non-specific changes in vessel width due to the resultant inflammatory response; therefore, their BVD was normalized for vessel width. To confirm increased vascularization, total vessel length was also measured per image.

Measurement of blood brain barrier permeability

Vessel leakage was evaluated by jugular vein injection of sulfo-NHS-biotin (0.07 mg/g, Pierce) 30 min pre-sacrifice. Four coronal sections were stained with streptavidin-conjugated Alexa 555 or Cy-5 (1:500, Jackson ImmunoResearch) and leakage area measured on confocal images using a Zeiss LSM Image browser.

Sequestration of human VEGF with Avastin

Avastin (Bevacizumab, Genentech) 4 mg/kg in saline was injected into the peritoneal cavity every other day[29] starting transplantation day. Human IgG (Sigma) was the control.

Microvessel isolation and western blot

Ipsilesional cortical tissue was minced (after removing meninges and large surface vessels), mixed with 30% dextran (Sigma) in Earle's Balanced Salt Solution (EBSS, GIBCO), centrifuged (3220g, 10 min, 4°C), the pellet washed in EBSS, re-pelleted, resuspended in 1ml EBSS, and passed through a 70µm then 40µm cell strainer (BD Falcon). Microvessels were collected from the 40µm strainer membrane, washed in EBSS, re-pelleted at 110g, resuspended, and sonicated in 1X lysis buffer (Cell Signaling Technology) containing phosphatase (Sigma) and protease inhibitors (Roche). 1 – 5µg of protein (equal loading per gel, per experiment) underwent SDS PAGE using 3–8% NuPAGE Tris-acetate gels (Invitrogen) and the gels blotted to polyvinylidene difluoride membranes (Invitrogen). The membranes were incubated with primary antibody, 4°C overnight: rabbit anti-phospho VEGFR2 (1:500, Millipore), rabbit anti-Tie 2 (1: 2000, Calbiochem), mouse anti-Occludin (1:500, BD Biosciences), rabbit anti-Zo-1 (1:250, Invitrogen), mouse anti-Claudin-5 (1:3000, Lifespan), mouse anti-actin (1:10000, Sigma). Secondary anti-mouse (1:2000) or anti-rabbit antibodies (1:3000, Cell Signaling Technology) were incubated 1h at room temperature, and a 5 min SuperSignal® West Pico (Thermo) incubation followed. The film was developed, and band intensity measured with Image J.

Behavior analysis

Ten trials of the vibrissae-evoked forelimb placing test was done on each side as described previously [30]. Behavior was tested pre-operatively for baseline performance and repeated weekly for 5 weeks post-dMCAo (blinded). Animals were excluded if their post-stroke score did not decrease 10% or more from baseline.

Statistics

Data are presented as means + SEM. Data were tested for normality and equal standard deviations in GraphPad InStat to determine the appropriate statistical test (parametric versus non-parametric). The text and figure legends describe the statistical tests; unless stated differently, all tests were two-tailed. Differences were considered statistically significant at $P < 0.05$.

RESULTS

hCNS-SCNs prevent secondary cortical damage and enhance functional recovery in an hVEGF-dependent manner

hCNS-SCNs were transplanted in the rat cortex 1 week post-stroke and successful engraftment was observed (Figure 1A, Supplementary Figures 1 and 7), consistent with our previous studies with these cells [27, 31]. Also consistent with our previous studies and that of others [32, 33], the cells migrated towards the lesion (Figure 1A). The cells started migrating by 2 weeks post-transplantation but did not reach the lesion edge until 3 to 4 weeks post-transplantation.

The barrel field cortex, a somatosensory cortical region coding for whisker displacement, was consistently damaged by the lesion, therefore a whisker stimulation test was employed to determine the effect of hCNS-SCNs on functional recovery [30]. Whisker-evoked paw reaching was significantly inhibited after stroke when the whiskers on the affected side (contralesional) (Figure 1B), but not the unaffected side (Supplemental Figure 2A), were stimulated. The affected whisker-paw response showed significantly greater recovery in cell-treated versus buffer-treated animals (Figure 1B). Cell-induced recovery was significant as early as 1 week post-transplantation, which is before the cells have migrated to the lesion. A 'dead hCNS-SCNs' control group did not induce recovery (Supplementary Figure 2C, D) implying that viable cells were necessary for efficacy.

Expression of human VEGF (hVEGF) by hCNS-SCNs was confirmed in vitro by ELISA (1.5ng/mg protein, minimum) and in vivo by immunofluorescent staining (Figure 1E, Supplementary Figure 1). Avastin was injected to neutralize stem cell-secreted hVEGF in vivo and some Avastin staining was observed in the parenchyma around the graft and also associated with blood vessels in the penumbra (Supplementary Figure 3). Avastin is an anti-human VEGF antibody that does not bind rodent VEGF [34]. Therefore, Avastin selectively inhibits the human VEGF secreted by the stem cells without affecting the host rodent VEGF. Avastin treatment significantly inhibited hCNS-SCNs-enhanced functional recovery (Figure 1C). Some inhibition was observed as early as 1 week post-treatment with Avastin; however, it was not significant until 3 weeks post-treatment (Figure 1C). The Avastin effect was specific as treatment with a control antibody, IgG, had no effect and Avastin did not affect functional recovery in the buffer-treated animals (Supplemental Figure 2B). However, given the small degree of recovery in the buffer animals, Avastin-induced inhibition would be very small and possibly below the sensitivity of our assay.

The remaining ipsilesional cortex was significantly larger in the cell-treated group compared to the buffer group at 4 weeks post-transplantation (Figure 1D), and a more healthy tissue architecture was apparent in the peri-infarct cortex of cell-treated animals (Supplementary Figure 4). Treatment with Avastin reduced this effect (Figure 1D, Supplementary Figure 4). This implies the cells reduce cortical atrophy that occurs at later stages after stroke, and this is dependent on hVEGF secretion.

hCNS-SCNs enhance BBB integrity and neovascularization after stroke with different kinetics

Blood brain barrier (BBB) integrity, which is critical for proper brain function, is disrupted after stroke lasting up to several weeks [35, 36]. To determine the effect of hCNS-SCNs on BBB permeability, a small molecule, biotin, was injected intravenously. hCNS-SCNs-treated animals exhibited significantly less leakage of biotin into the peri-infarct parenchyma compared to buffer-treated animals (Figure 2A, B), implying that hCNS-SCNs enhance BBB integrity. This was an early host response to hCNS-SCNs observed at 1 week post-transplantation; a similar trend was observed at 2 weeks post-transplantation.

To investigate the effect of hCNS-SCNs on neovascularization, the density of lectin-perfused vessels (blood vessel density: BVD) was analyzed in 3 cortical regions of interest (ROIs): the peri-infarct (ROI1), near the graft (ROI3), and between the two (ROI2) (Figure 2C). Cell-treated animals exhibited enhanced neovascularization after ischemia compared to buffer-treated animals (Figure 2D, E); this observation was limited to the ipsilesional hemisphere with no effect in the contralesional side (Supplementary Figure 5A). hCNS-SCNs-induced effects on vascularization were under spatial regulation and most pronounced in the peri-infarct region as opposed to ROIs closer to the graft (Figure 2E). This implies that the peri-infarct microenvironment is responsive to hCNS-SCNs while the more healthy tissue is less permissive. However, a trend for smaller increases in vasculature that approached significance was observed in the other ROIs at later time points.

In addition to the spatial control, temporal regulation of hCNS-SCNs-induced effects on vessel growth was observed. There was no observed effect on vessel density at 1 week post-transplantation when the cells elicit their effect on BBB integrity. The most pronounced effect of the cells in the peri-infarct cortex occurred later at 2 weeks post-transplantation and declined thereafter (Figure 2E). Increased vascularization at 2 weeks was also confirmed by vessel length measurements (Supplemental Figure 5B). This timing mirrors the increase in vasculature observed in stroke-only animals, which peaks at 3 weeks post-stroke (equivalent to 2 weeks post-transplantation; slope coefficient wk1–wk3 post-stroke = 0.16, $p < 0.05$; Supplemental Figure 5C).

Transplanted hCNS-SCNs are very closely associated with vessels (Supplemental Figure 6) ideally situated to influence the vasculature. However, they are distant from the peri-infarct cortex when they elicit their maximum effect on the vasculature (at 1 and 2 weeks post-transplantation), only migrating to this region at 3 and 4 weeks post-transplantation (Figure 1). Therefore, hCNS-SCNs function remotely to enhance peri-infarct vascular regeneration. This is in contrast to other reports that show transplanted cells act locally to enhance vascularization [12–14].

hVEGF secretion is required for hCNS-SCNs-induced neovascularization, but not BBB repair

Avastin treatment significantly reduced hCNS-SCNs-enhanced neovascularization in the peri-infarct cortex as determined both by vessel density (Figure 3A, B) and vessel length analysis (Supplemental Figure 5B). This effect was not seen in buffer-treated animals confirming that Avastin did not block rodent VEGF. Furthermore, the IgG control had no effect on either hCNS-SCNs- or buffer-treated groups, and Avastin did not adversely affect cell survival (Supplemental Figure 7B; percent cell survival 5.5 ± 1.5 (Avastin) versus 6.9 ± 2.7 (IgG)). There was also no obvious effect of Avastin on hCNS-SCNs differentiation; however this was not quantifiable given the density of the graft at this time (Supplemental Figure 7C, D). Together, these data confirm that the effects of Avastin were specific to its neutralization of hVEGF. Thus, VEGF secretion by the transplanted cells is essential for

increased vascularization. In contrast, Avastin had no effect on hCNS-SCns-induced BBB integrity (Figure 3A, C) implying an hVEGF-independent effect of the cells on this parameter.

hCNS-SCns enhance angiogenic signaling pathways

Vascular regeneration and remodeling is regulated in part by signaling through the two main pro-angiogenic receptors VEGFR2 (Flk1) and Tie2, whose ligands are VEGF and Angiopoietin 1 & 2 respectively. Western blot analysis of cortical microvessels isolated at 1 week post-transplantation revealed that hCNS-SCns-treated animals exhibit enhanced phosphorylation of the VEGFR2 compared to the buffer group, indicative of increased signaling through the receptor (Figure 4A, B: the same trend was observed with cell- and buffer-only treated animals, i.e., no antibody treatment, data not shown). Avastin blocked the cell-induced phosphorylation of VEGFR (with no effect in buffer-treated animals), implying a role of secreted hVEGF. Furthermore, hCNS-SCns also significantly enhanced expression of the angiopoietin receptor Tie2 at 1 week post-transplantation in cell-only versus buffer-only treated groups (buffer vs. cell (band intensity): 0.97 \pm 0.2 vs. 3.1 \pm 0.6, $p < 0.01$, Supplemental Figure 8). The same trend was observed in cell and buffer IgG-treated animals and blocked by Avastin (Figure 4A, B); however, statistical significance was not reached in either case.

hCNS-SCns enhance tight junction and β -dystroglycan protein expression after stroke

Tight junctions (TJs) between endothelial cells are critical for BBB integrity, and are formed by TJ proteins [37, 38]. Western blot analysis of microvessels isolated from the ischemic cortex of hCNS-SCns-treated animals at 1 week post-transplantation revealed significant increased expression of the TJ proteins occludin and claudin-5, but no change in ZO-1 expression compared to the buffer group (Figure 4C, D: similarly observed with cell- and buffer-only treated animals, data not shown). This is consistent with increased BBB integrity in cell-treated animals at this time. Surprisingly, the addition of Avastin significantly reduced the hCNS-SCns-induced expression of occludin and claudin 5 in cell-treated animals (Figure 4C, D) without an apparent change in BBB leakage (Figure 3C); however, occludin expression did remain significantly higher in cell/Avastin-treated versus buffer/Avastin-treated animals ($p < 0.05$ cell/Avastin versus buffer/Avastin).

Astrocytic end-feet surrounding the vessels also contribute to BBB integrity [37, 39] and dystroglycan (DG), which binds astrocytes to the endothelial cell extracellular matrix, may be involved [40–42]. DG appears to be associated with all microvessels in the cortex (Supplemental Figure 9) and, at least in larger vessels, colocalized with the astrocytic end-foot marker aquaporin-4 rather than endothelial cells (Figure 5A, C). hCNS-SCns enhanced expression of the α subunit of DG (α -DG) after stroke (Figure 5D). However, this was not observed at 1 week post-transplantation when the cells elicit their effect on BBB integrity, indicating that enhanced α -DG expression is not involved in the initial cell-induced repair of the BBB. α -DG expression exhibited a similar spatio-temporal pattern as observed for lectin staining of blood vessels (compare Figs. 2E and 5D), with the most significant increase in expression in the peri-infarct cortex (ROI 1 Figure 5D) starting at 2 weeks post-transplantation. Furthermore, Avastin blocked the cell-induced expression of α -DG (Figure 5E), implying a role of hVEGF in this effect.

hCNS-SCns decrease the inflammatory response after stroke

hCNS-SCns-treated animals had significantly fewer Iba1-positive monocytes/macrophages in the peri-infarct cortex than buffer-treated animals at 1 week post-transplantation and a similar trend was measured at 2 weeks post-transplantation (Figure 6A, B); no significant difference in IBA1-positive cells between buffer- and hCNS-SCns-treated animals was

observed in the rest of the cortex (ROI2). hCNS-SCns treatment also reduced the number of IBA1-positive cells in IgG-injected animals compared to buffer-treated animals (Figure 6C); this immunomodulation was blocked by Avastin treatment, implying that hVEGF is important for this immunomodulatory effect. The cells could not fully suppress the inflammatory response induced by adding IgG (compare cell/IgG with cell-only); this is likely because the inflammatory response is too great. However, the fact that the cells had a measurable suppressive effect even in the presence of such a large inflammatory response implies they have significant immunomodulatory properties.

Correlating hCNS-SCns-induced changes in the brain with functional recovery

We compared the timing of hCNS-SCns-induced recovery to cell-induced changes in the brain and found that, although vascularization is postulated to be important for recovery after stroke, significant recovery was observed before effects on the vasculature were seen (Figure 7A). This early phase of recovery (at 2 weeks post-stroke, i.e., 1 week post-transplantation) correlated with hCNS-SCns-induced changes in inflammation and BBB integrity. This raises the question whether hCNS-SCns-enhanced recovery is based solely on these early events (i.e., BBB and inflammation changes) and whether neovascularization is involved at all. However, an interesting observation about the pattern of recovery hints that neovascularization may be important for recovery at later time points: examination of all the individual cell-treated animals revealed two distinct groups with respect to recovery patterns. Group I exhibited early recovery within the first week of transplantation before vascularization; Group II exhibited delayed recovery starting in the third week post-transplantation coincident with neovascularization (Figure 7B). In contrast, buffer-treated animals exhibited a more random recovery pattern commencing at all time points post-stroke (data not shown). Furthermore, Avastin, which inhibits hCNS-SCns-induced vascularization, clearly inhibits recovery in Group II (compare group II, Figures 7B, C).

Taken together, our data demonstrate that hCNS-SCns influence multiple parameters of brain repair after stroke with different temporal profiles as summarized in the schematic (Figure 7D), and that these effects are mediated, at least in part, by secretion of hVEGF.

DISCUSSION

We show that hVEGF secretion by transplanted hCNS-SCns is directly involved in the functional recovery they elicit *in vivo*, as Avastin, which neutralizes human but not rodent VEGF, inhibited the hCNS-SCns-induced improvements we observed. Others have reported that overexpression of VEGF in transplanted cells further enhances recovery [8, 9]. However, in these studies it is unclear if VEGF acts directly on the host brain or indirectly by enhancing graft survival. Thus, such studies do not distinguish whether VEGF is necessary for recovery or alternatively amplifies recovery induced by some other mechanism. This study therefore provides the first direct evidence of a stem cell-secreted factor that is critical for cell-induced functional recovery in the post-stroke brain.

Having established a critical role for secreted hVEGF in functional recovery, we then investigated what changes hCNS-SCns elicit in the brain to enhance recovery and, in particular, which of these changes are modulated by hVEGF. We and others [12–14, 43] have postulated a role for stem cell-induced vascularization in cell-induced recovery; this fits with the essential role of hVEGF in recovery as we show the first *in vivo* evidence that the induced vascularization is hVEGF-dependent. We also demonstrate for the first time that hCNS-SCns-induced neovascularization is regulated in a spatio-temporal manner. The most significant increase was observed in the peri-infarct region at 2 weeks post-transplantation, with very little effect in areas closer to the graft. This implies an effect that is not simply a uniform response to a gradient of graft-secreted factors, but one that requires host tissue

responsiveness to the graft. Therapeutically this is important as it shows hCNS-SCNs do not readily affect vascularization in healthy tissue but primarily influence tissue already undergoing repair and re-vascularization. Furthermore, hCNS-SCNs-treated animals demonstrate a profile of vessel induction followed by regression suggesting a highly regulated process rather than a continuous, aberrant, and potentially detrimental increase in blood vessel formation as is observed in certain retinopathies.

The peri-infarct tissue is presumably the most responsive region to hCNS-SCNs as this area upregulates angiogenic signaling after ischemia through the VEGFR2 and the angiopoietin receptors Tie 1 and 2 [44]. We found that hCNS-SCNs treatment increases endothelial cell signaling through VEGFR2 and increases Tie2 expression *in vivo* prior to the observed changes in vascularization. Furthermore, we demonstrated for the first time *in vivo* that secretion of hVEGF by hCNS-SCNs is both necessary and sufficient for the increased angiogenic signaling as it was abolished by Avastin. In addition to changes in the blood vessel number, we found that hCNS-SCNs also enhances expression of α -dystroglycan in a hVEGF-dependent manner. α -dystroglycan is an extracellular matrix adhesion protein abundant in astrocytic endfeet surrounding blood vessels that may also be expressed by pericytes and endothelial cells [40, 45]. Thus, this data implies that the hCNS-SCNs affect not only endothelial cells but also other critical components of the vasculature, which may be indicative of enhanced communication and functioning of the neurovascular unit [46].

The exact contribution of enhanced neovascularization to stem cell-induced functional recovery is unclear as VEGF is known to have pleiotropic effects, including influencing neurite outgrowth and neurogenesis (reviewed in [47]), all of which could contribute to hVEGF-induced functional recovery. What is apparent from our study is that neovascularization is unlikely to be involved in the initial phase of recovery, as hCNS-SCNs significantly enhanced behavior recovery at 1 week post-transplantation, which is prior to their effects on vessel formation. Omori et al. [48] also concluded that angiogenesis was not the only contributing factor for human mesenchymal stem cell (hMSC)-induced functional recovery, as different hMSC treatments resulted in different levels of functional recovery but had similar effects on angiogenesis.

The early cell-induced recovery at 1 week post-transplantation instead coincided with hCNS-SCNs effects on inflammation and BBB repair. Previous studies have reported on the unexpected anti-inflammatory effects of neural stem cells or MSCs and their ability to improve BBB integrity [49, 50] when administered either before or acutely (6 – 72h) after stroke [21–24]. Our study expands this therapeutic window and demonstrates that sub-acute delivery of hCNS-SCNs remains immunosuppressive and can restore impaired BBB function. While the T cell deficiency of our Nude rat model could potentially bias the inflammatory data, this situation is not unlike that of the patient as they will be given immunosuppressive drugs to inhibit T cells to prevent neural graft rejection.

It is not understood how xenografts of human stem cells into rodents are immunosuppressive; our data demonstrates for the first time that secretion of hVEGF plays an important role in this immunomodulatory effect of hCNS-SCNs. This was unexpected as VEGF is conventionally considered to be pro-inflammatory. However, a growing body of literature corroborates the anti-inflammatory properties of VEGF. Manoonkitiwingsa [51] found that treatment of ischemic brains with low doses of VEGF reduced macrophage numbers, while higher doses increased macrophage density. Furthermore, hematopoietic progenitor cells express VEGF receptors and VEGF has been shown to directly inhibit the growth of myeloid progenitor cells (the monocyte and granulocyte precursors) [52]. Additionally, VEGF reportedly suppresses the development and activation of dendritic cells (antigen presenting cells important in initiating immune responses) and T cells [53, 54]. Pre-

clinical and clinical studies indicate that the immunosuppressive effect of VEGF may be involved in establishing immune privilege of VEGF-secreting tumors [55]. Thus, precedence exists for an immunosuppressive role for VEGF, which may be dependent on the dose, timing, and route of VEGF delivery, suggesting the importance of further investigation of VEGF in the context of cerebral ischemia and cell transplantation.

The immunosuppressive effects of hCNS-SCNs may contribute to hCNS-SCNs-induced BBB repair as inflammation contributes to BBB breakdown [18, 19, 38], and there is significant cross-talk between inflammatory cells and components of the neurovascular unit [20]. Additionally, hCNS-SCNs enhanced other effectors of the BBB including increased expression of Tie2 and TJ proteins. A similar result was reported by Zacharek [50] after acute delivery of MSCs, implying this effect is independent of the cell type transplanted. Avastin blocked both hCNS-SCNs-induced immunomodulation and TJ expression; these may be interrelated as inflammation is known to affect TJ proteins expression [38]. However, although hVEGF secretion was important for these aforementioned parameters, cell-enhanced BBB integrity appeared to be hVEGF-independent as it was not blocked by Avastin. A possible explanation for this disparity is that occludin expression, although reduced in the presence of Avastin, still remained significantly elevated in cell-treated animals compared to the buffer control group, and perhaps retaining a certain threshold level of occludin may be enough for sustained BBB integrity. It remains to be determined whether transcellular influx (i.e., through the endothelial cells) of biotin through its known transporter [56] or by pinocytosis is also affected in our experimental paradigm, as such mechanisms are less influenced by TJs than paracellular leakage (i.e., between endothelial cells).

Understanding how cell transplantation affects the host brain will lead to further improvements in cell efficacy and, perhaps more importantly, may highlight potential side effects of cell therapy. Furthermore, cell-induced changes in the brain could serve as useful surrogate clinical indicators of transplanted cell activity. For example, changes in vasculature and blood flow can be measured non-invasively in patients by perfusion studies. Moving from the bench to the clinic also raises cell manufacturing issues, in particular designing bioassays to predict clinical efficacy of the cell product [57]. Understanding the mechanism of action of the transplanted cells will be critical for this and our data implies that secreted VEGF could be an important predictive marker of efficacy, especially as cell viability may affect the capacity of stem cells to secrete VEGF and other potential biofactors. However, future studies are required to determine the relationship between the amount of hVEGF secreted and the extent of cell-induced recovery.

CONCLUSION

In summary, we established that stem cell-secreted VEGF is essential for hCNS-SCNs-induced recovery; no doubt other secreted factors will also be involved. Furthermore, functional recovery correlated with hCNS-SCNs-induced suppression of inflammation, increased vessel formation, and enhanced BBB integrity; hVEGF was important for the immunosuppressive and neovascularization effects of the hCNS-SCNs, and may possibly be involved in altering BBB integrity. Thus, sub-acute cell transplantation therapy offers a multi-modal strategy for brain repair that could significantly expand the therapeutic window for stroke. Finally, as vascular degeneration and inflammation are hallmarks of many other cerebral pathologies [37] including meningitis, multiple sclerosis, and vascular dementia, further research focused on the vascular repair and immunosuppressive properties of transplanted cells could have far reaching implications as stem cell therapies are developed and advanced to the clinic.

Supplementary Material

Refer to Web version on PubMed Central for supplementary material.

Acknowledgments

Funding: This work was supported by National Institutes of Health National Institute of Neurological Disorders and Stroke [NS058784, NS27292, NS37520 to G.K.S.], the William Randolph Hearst Foundation, Bernard and Ronni Lacroute, Russell and Elizabeth Siegelman, and the Edward E. Hills Fund (to G.K.S.); M.P.P. is a recipient of a postdoctoral fellowship from the Ministry of Education and Science of Spain (reference 2007-1219).

We would like to thank Calvin Kuo, Richard Daneman, Carolina Maier, Pak Chan, Marion Buckwalter, Katrin Andreasson, and Napoleone Ferrara for helpful discussions. Thanks to Purnima Narasimhan and Dongping He for technical assistance, Alexandra Capela, Cindy Samos, and Bruce Schaar for comments on the manuscript, and Beth Hoyte for help with the figures.

References

1. Borlongan CV, Tajima Y, Trojanowski JQ, et al. Transplantation of cryopreserved human embryonal carcinoma-derived neurons (NT2N cells) promotes functional recovery in ischemic rats. *Exp Neurol*. 1998; 149:310–321. [PubMed: 9500961]
2. Chen J, Sanberg PR, Li Y, et al. Intravenous administration of human umbilical cord blood reduces behavioral deficits after stroke in rats. *Stroke*. 2001; 32:2682–2688. [PubMed: 11692034]
3. Hicks AU, Lappalainen RS, Narkilahti S, et al. Transplantation of human embryonic stem cell-derived neural precursor cells and enriched environment after cortical stroke in rats: cell survival and functional recovery. *Eur J Neurosci*. 2009; 29:562–74. [PubMed: 19175403]
4. Stroemer P, Hope A, Patel S, et al. Development of a human neural stem cell line for use in recovery from disability after stroke. *Front Biosci*. 2008; 13:2290–2. [PubMed: 17981710]
5. Bliss T, Guzman R, Daadi M, et al. Cell transplantation therapy for stroke. *Stroke*. 2007; 38:817–826. [PubMed: 17261746]
6. Guzman R, Choi R, Gera A, et al. Intravascular cell replacement therapy for stroke. *Neurosurg Focus*. 2008; 24:E15. [PubMed: 18341391]
7. clinicaltrials.gov Identifier: NCT00473057; NCT00859014; NCT00535197; NCT00950521. 2009.
8. Lee HJ, Kim KS, Park IH, et al. Human neural stem cells over-expressing VEGF provide neuroprotection, angiogenesis and functional recovery in mouse stroke model. *PLoS ONE*. 2007; 2:e156. [PubMed: 17225860]
9. Miki Y, Nonoguchi N, Ikeda N, et al. Vascular endothelial growth factor gene-transferred bone marrow stromal cells engineered with a herpes simplex virus type 1 vector can improve neurological deficits and reduce infarction volume in rat brain ischemia. *Neurosurgery*. 2007; 61:586–94. discussion 594–5. [PubMed: 17881973]
10. Krupinski J, Kaluza J, Kumar P, et al. Prognostic value of blood vessel density in ischaemic stroke. *Lancet*. 1993; 342:742. [PubMed: 8103843]
11. Senior K. Angiogenesis and functional recovery demonstrated after minor stroke. *Lancet*. 2001; 358:817. [PubMed: 11564497]
12. Onda T, Honmou O, Harada K, et al. Therapeutic benefits by human mesenchymal stem cells (hMSCs) and Ang-1 gene-modified hMSCs after cerebral ischemia. *J Cereb Blood Flow Metab*. 2008; 28:329–40. [PubMed: 17637706]
13. Taguchi A, Soma T, Tanaka H, et al. Administration of CD34+ cells after stroke enhances neurogenesis via angiogenesis in a mouse model. *J Clin Invest*. 2004; 114:330–338. [PubMed: 15286799]
14. Chen J, Zhang ZG, Li Y, et al. Intravenous administration of human bone marrow stromal cells induces angiogenesis in the ischemic boundary zone after stroke in rats. *Circ Res*. 2003; 92:692–699. [PubMed: 12609969]
15. Hayashi T, Deguchi K, Nagotani S, et al. Cerebral ischemia and angiogenesis. *Curr Neurovasc Res*. 2006; 3:119–129. [PubMed: 16719795]

16. Slevin M, Kumar P, Gaffney J, et al. Can angiogenesis be exploited to improve stroke outcome? Mechanisms and therapeutic potential. *Clin Sci (Lond)*. 2006; 111:171–83. [PubMed: 16901264]
17. Lok J, Gupta P, Guo S, et al. Cell-cell signaling in the neurovascular unit. *Neurochem Res*. 2007; 32:2032–2045. [PubMed: 17457674]
18. Abbott NJ. Inflammatory mediators and modulation of blood-brain barrier permeability. *Cell Mol Neurobiol*. 2000; 20:131–47. [PubMed: 10696506]
19. McColl BW, Rothwell NJ, Allan SM. Systemic inflammation alters the kinetics of cerebrovascular tight junction disruption after experimental stroke in mice. *J Neurosci*. 2008; 28:9451–62. [PubMed: 18799677]
20. del Zoppo GJ. Inflammation and the neurovascular unit in the setting of focal cerebral ischemia. *Neuroscience*. 2009; 158:972–82. [PubMed: 18824084]
21. Lee ST, Chu K, Jung KH, et al. Anti-inflammatory mechanism of intravascular neural stem cell transplantation in haemorrhagic stroke. *Brain*. 2008; 131:616–29. [PubMed: 18156155]
22. Vendrame M, Gemma C, de Mesquita D, et al. Anti-inflammatory effects of human cord blood cells in a rat model of stroke. *Stem Cells Dev*. 2005; 14:595–604. [PubMed: 16305344]
23. Ohtaki H, Ylostalo JH, Foraker JE, et al. Stem/progenitor cells from bone marrow decrease neuronal death in global ischemia by modulation of inflammatory/immune responses. *Proc Natl Acad Sci U S A*. 2008; 105:14638–43. [PubMed: 18794523]
24. Bacigaluppi M, Pluchino S, Jametti LP, et al. Delayed post-ischaemic neuroprotection following systemic neural stem cell transplantation involves multiple mechanisms. *Brain*. 2009; 132:2239–51. [PubMed: 19617198]
25. Pluchino S, Zanotti L, Rossi B, et al. Neurosphere-derived multipotent precursors promote neuroprotection by an immunomodulatory mechanism. *Nature*. 2005; 436:266–71. [PubMed: 16015332]
26. Vos JG, Kreeftenberg JG, Kruijt BC, et al. The athymic nude rat. II. Immunological characteristics. *Clin Immunol Immunopathol*. 1980; 15:229–37. [PubMed: 6986220]
27. Kelly S, Bliss TM, Shah AK, et al. Transplanted human fetal neural stem cells survive, migrate, and differentiate in ischemic rat cerebral cortex. *Proc Natl Acad Sci U S A*. 2004; 101:11839–11844. [PubMed: 15280535]
28. Uchida N, Buck DW, He D, et al. Direct isolation of human central nervous system stem cells. *Proc Natl Acad Sci U S A*. 2000; 97:14720–14725. [PubMed: 11121071]
29. Rubenstein JL, Kim J, Ozawa T, et al. Anti-VEGF antibody treatment of glioblastoma prolongs survival but results in increased vascular cooption. *Neoplasia*. 2000; 2:306–314. [PubMed: 11005565]
30. Woodlee MT, Asseo-Garcia AM, Zhao X, et al. Testing forelimb placing “across the midline” reveals distinct, lesion-dependent patterns of recovery in rats. *Exp Neurol*. 2005; 191:310–7. [PubMed: 15649486]
31. Guzman R, Uchida N, Bliss TM, et al. Long-term monitoring of transplanted human neural stem cells in developmental and pathological contexts with MRI. *Proc Natl Acad Sci U S A*. 2007; 104:10211–6. [PubMed: 17553967]
32. Imitola J, Raddassi K, Park KI, et al. Directed migration of neural stem cells to sites of CNS injury by the stromal cell-derived factor 1alpha/CXC chemokine receptor 4 pathway. *Proc Natl Acad Sci U S A*. 2004; 101:18117–18122. [PubMed: 15608062]
33. Ohab JJ, Fleming S, Blesch A, et al. A neurovascular niche for neurogenesis after stroke. *J Neurosci*. 2006; 26:13007–13016. [PubMed: 17167090]
34. Ferrara N, Hillan KJ, Gerber HP, et al. Discovery and development of bevacizumab, an anti-VEGF antibody for treating cancer. *Nat Rev Drug Discov*. 2004; 3:391–400. [PubMed: 15136787]
35. Veltkamp R, Siebing DA, Sun L, et al. Hyperbaric oxygen reduces blood-brain barrier damage and edema after transient focal cerebral ischemia. *Stroke*. 2005; 36:1679–1683. [PubMed: 16020761]
36. Yu SW, Friedman B, Cheng Q, et al. Stroke-evoked angiogenesis results in a transient population of microvessels. *J Cereb Blood Flow Metab*. 2007; 27:755–763. [PubMed: 16883352]
37. Zlokovic BV. The blood-brain barrier in health and chronic neurodegenerative disorders. *Neuron*. 2008; 57:178–201. [PubMed: 18215617]

38. Sandoval KE, Witt KA. Blood-brain barrier tight junction permeability and ischemic stroke. *Neurobiol Dis.* 2008; 32:200–19. [PubMed: 18790057]
39. Abbott NJ, Ronnback L, Hansson E. Astrocyte-endothelial interactions at the blood-brain barrier. *Nat Rev Neurosci.* 2006; 7:41–53. [PubMed: 16371949]
40. Milner R, Hung S, Wang X, et al. The rapid decrease in astrocyte-associated dystroglycan expression by focal cerebral ischemia is protease-dependent. *J Cereb Blood Flow Metab.* 2008; 28:812–23. [PubMed: 18030304]
41. Nico B, Frigeri A, Nicchia GP, et al. Severe alterations of endothelial and glial cells in the blood-brain barrier of dystrophic mdx mice. *Glia.* 2003; 42:235–251. [PubMed: 12673830]
42. Winder SJ. The complexities of dystroglycan. *Trends Biochem Sci.* 2001; 26:118–124. [PubMed: 11166570]
43. Shyu WC, Lin SZ, Chiang MF, et al. Intracerebral peripheral blood stem cell (CD34+) implantation induces neuroplasticity by enhancing beta1 integrin-mediated angiogenesis in chronic stroke rats. *J Neurosci.* 2006; 26:3444–3453. [PubMed: 16571751]
44. Zhang ZG, Zhang L, Tsang W, et al. Correlation of VEGF and angiopoietin expression with disruption of blood-brain barrier and angiogenesis after focal cerebral ischemia. *J Cereb Blood Flow Metab.* 2002; 22:379–392. [PubMed: 11919509]
45. Zaccaria ML, Di Tommaso F, Brancaccio A, et al. Dystroglycan distribution in adult mouse brain: a light and electron microscopy study. *Neuroscience.* 2001; 104:311–24. [PubMed: 11377836]
46. del Zoppo GJ, Milner R. Integrin-matrix interactions in the cerebral microvasculature. *Arterioscler Thromb Vasc Biol.* 2006; 26:1966–75. [PubMed: 16778120]
47. Ruiz de Almodovar C, Lambrechts D, Mazzone M, et al. Role and therapeutic potential of VEGF in the nervous system. *Physiol Rev.* 2009; 89:607–48. [PubMed: 19342615]
48. Omori Y, Honmou O, Harada K, et al. Optimization of a therapeutic protocol for intravenous injection of human mesenchymal stem cells after cerebral ischemia in adult rats. *Brain Res.* 2008; 1236:30–8. [PubMed: 18722359]
49. Borlongan CV, Lind JG, Dillon-Carter O, et al. Bone marrow grafts restore cerebral blood flow and blood brain barrier in stroke rats. *Brain Res.* 2004; 1010:108–16. [PubMed: 15126123]
50. Zacharek A, Chen J, Cui X, et al. Angiopoietin1/Tie2 and VEGF/Flk1 induced by MSC treatment amplifies angiogenesis and vascular stabilization after stroke. *J Cereb Blood Flow Metab.* 2007; 27:1684–1691. [PubMed: 17356562]
51. Manoonkitiwongsa PS, Schultz RL, Whitter EF, et al. Contraindications of VEGF-based therapeutic angiogenesis: effects on macrophage density and histology of normal and ischemic brains. *Vascul Pharmacol.* 2006; 44:316–25. [PubMed: 16530019]
52. Broxmeyer HE, Cooper S, Li ZH, et al. Myeloid progenitor cell regulatory effects of vascular endothelial cell growth factor. *Int J Hematol.* 1995; 62:203–15. [PubMed: 8589366]
53. Gabrilovich DI, Chen HL, Girgis KR, et al. Production of vascular endothelial growth factor by human tumors inhibits the functional maturation of dendritic cells. *Nat Med.* 1996; 2:1096–103. [PubMed: 8837607]
54. Ohm JE, Gabrilovich DI, Sempowski GD, et al. VEGF inhibits T-cell development and may contribute to tumor-induced immune suppression. *Blood.* 2003; 101:4878–86. [PubMed: 12586633]
55. Ellis LM, Hicklin DJ. VEGF-targeted therapy: mechanisms of anti-tumour activity. *Nat Rev Cancer.* 2008; 8:579–91. [PubMed: 18596824]
56. Spector R, Johanson CE. Vitamin transport and homeostasis in mammalian brain: focus on Vitamins B and E. *J Neurochem.* 2007; 103:425–38. [PubMed: 17645457]
57. Kirouac DC, Zandstra PW. The systematic production of cells for cell therapies. *Cell Stem Cell.* 2008; 3:369–81. [PubMed: 18940729]

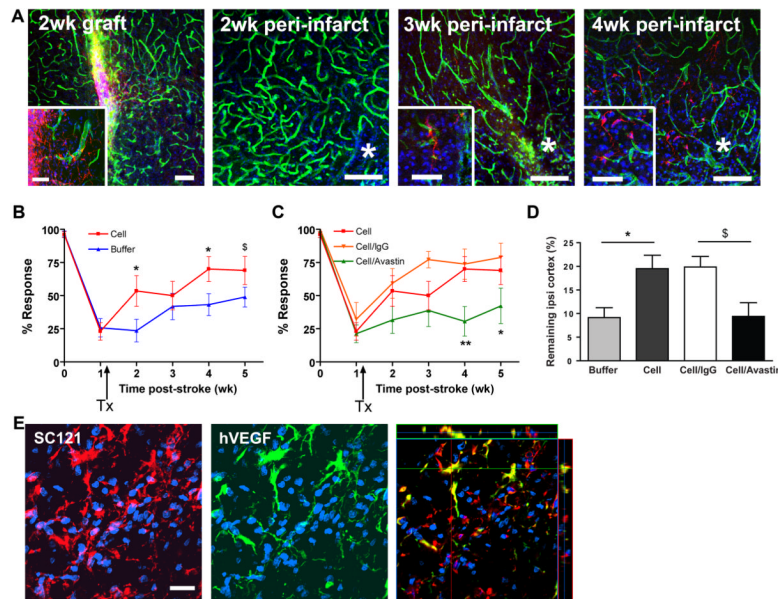


Figure 1. hCNS-SCns enhance functional recovery and reduce cortical atrophy in a hVEGF-dependent manner

(A) hCNS-SCns (red: human cytoplasmic marker SC121) survive and migrate over time; green: lectin-positive blood vessels; blue: DAPI. * indicates lesion. Inset: higher magnification of hCNS-SCns. Scale: 100 μ m (50 μ m in inset, except 3 wk inset: 25 μ m). (B) hCNS-SCns-treated animals (n=10) showed significantly improved behavioral recovery after stroke compared to buffer-treated animals (n=14). TX: transplantation. P=0.032 by repeated measures ANOVA; * p<0.05; \$ p=0.06 by t-test. (C) Avastin treatment significantly blocked hCNS-SCns-induced recovery. p=0.02 by repeated measures ANOVA between cell/Avastin and cell groups; * p<0.05; ** p<0.01 by t-test; cell/Avastin: n= 12-9; cell/IgG: n=7-4, (wk (0-3) - wk (4-5)). (D) The volume of the remaining ipsilesional cortex was significantly larger in hCNS-SCns-treated versus buffer-treated animals at 4 wk post-transplantation; this effect was blocked by Avastin. * p<0.05 by t-test; \$ p=0.06 by Mann-Whitney; n=4-5. (E) hCNS-SCns (red) express hVEGF (green). The anti-VEGF antibody is specific for human VEGF and does not cross react with rat VEGF Scale: 50 μ m.

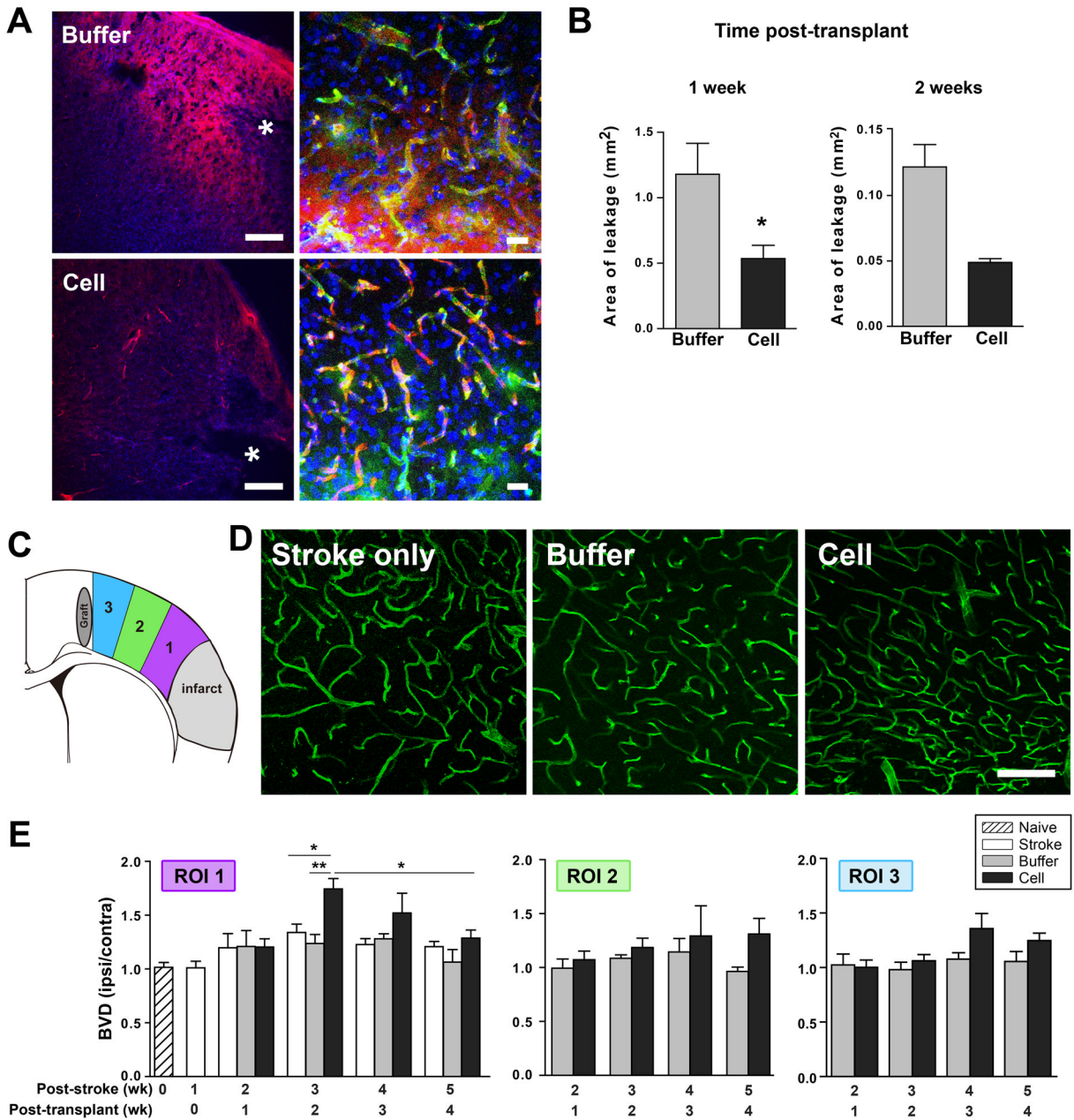


Figure 2. hCNS-SCNs enhance BBB integrity and neovascularization after stroke with different kinetics

(A) Confocal image at 1 wk post-transplantation illustrating less biotin leakage (red) in the peri-infarct area of cell- versus buffer-treated animals. Higher magnification: biotin leaks from vessels into the parenchyma in buffer- but not cell-treated animals. * indicates lesion. Scale: 200µm, 20µm in higher magnification images. (B) Quantification of biotin leakage; * p<0.05 by t-test. N= 5–6 at 1 wk; n=3 at 2 wk. (C) Schematic showing regions of interest (ROI) analyzed for blood vessel density. (D) Confocal images of lectin-perfused vessels in the peri-infarct cortex (ROI 1) at 2 wk post-transplantation. Scale: 100µm. (E) Quantification of the blood vessel density (BVD) in the ROIs over time. Cell-treated animals exhibit a general trend of enhanced neovascularization that is most pronounced in the peri-infarct area (ROI 1) at 2 wk post-transplantation; p=0.004 by one way ANOVA at 2

wk post-transplantation with * $p < 0.05$, ** $p < 0.01$ by Tukey post-hoc test. Comparison of cell group 2 & 4 wk post-transplant by Mann-Whitney test. Cell group: $n=6$ & buffer group: $n=4-5$ at 1 & 2 wk post-transplant; $n=3-5$ other groups.

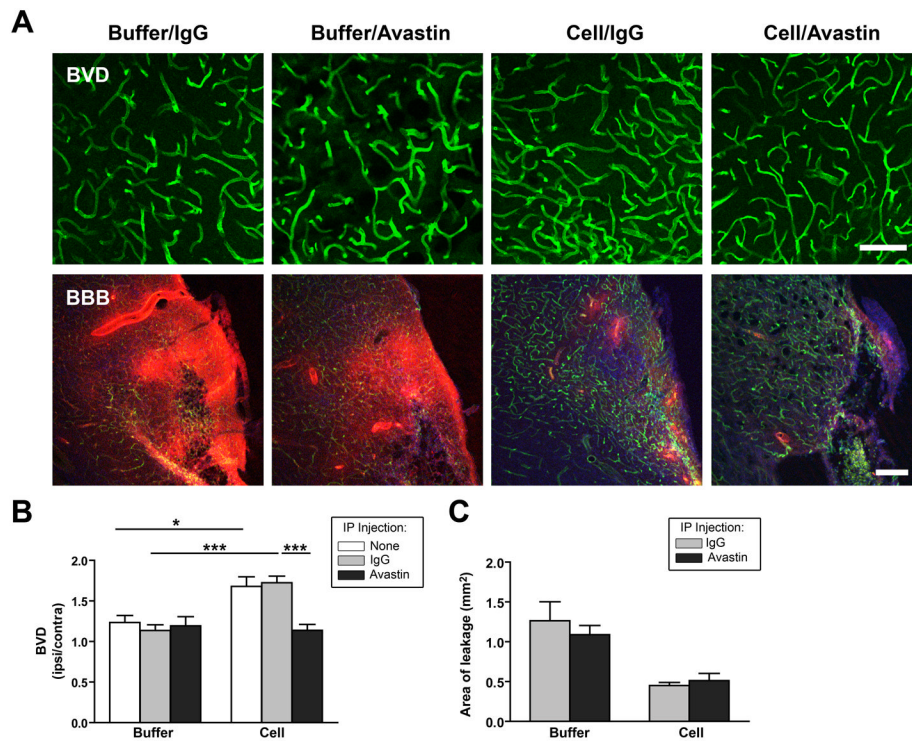


Figure 3. Avastin blocks cell-induced neovascularization but not BBB repair

(A) Confocal images showing blood vessel density (BVD) of lectin-stained blood vessels (green) and BBB leakage of biotin (red) at 2 wk after cell or buffer transplantation in animals treated with IgG or Avastin. Scale: BVD:100 μ m; BBB: 200 μ m. (B) Quantification revealed that Avastin blocks hCNS-SCns-enhanced vascularization; * $p < 0.05$; ** $p < 0.01$; *** $p < 0.001$ by t-test. $N = 4$ for buffer/Avastin, $n = 5-8$ for all other groups. (C) Avastin did not affect the relative BBB leakage of biotin in cell or buffer animals. $N = 5$ for IgG treated animals; $n = 3-4$ for Avastin-treated animals.

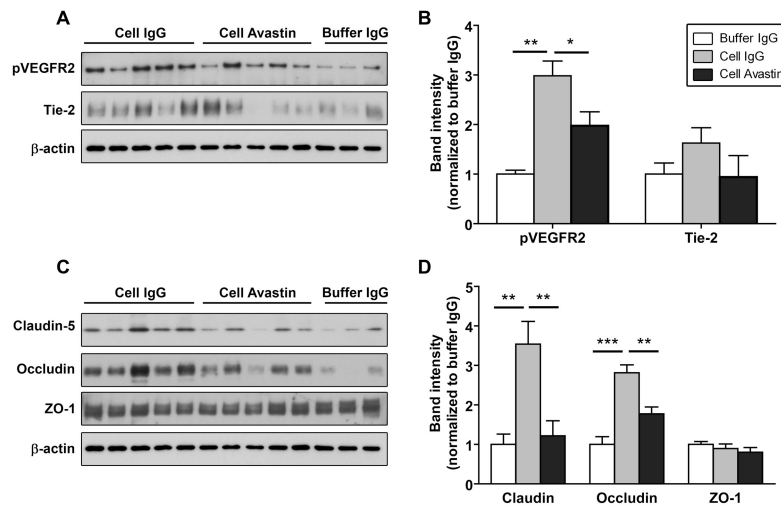


Figure 4. hCNS-SCNs increase expression of angiogenic receptors and tight junction proteins (A & C) Representative Western blot analysis of ipsilesional cortical microvessels isolated from brains at 1 wk post-transplantation. (B & D) Quantification of the Western blots for the relative expression of angiogenic receptors (B) and tight junction proteins (D). Cell-treated animals show enhanced expression of pVEGFR2, Tie-2, claudin 5 and occludin, and this is blocked by Avastin treatment. Note: the buffer/Avastin group is omitted for clarity but did not differ from the buffer/IgG group. Buffer groups: n=6, cell groups: n=5. * $p < 0.05$; *** $p < 0.001$ by t-test.

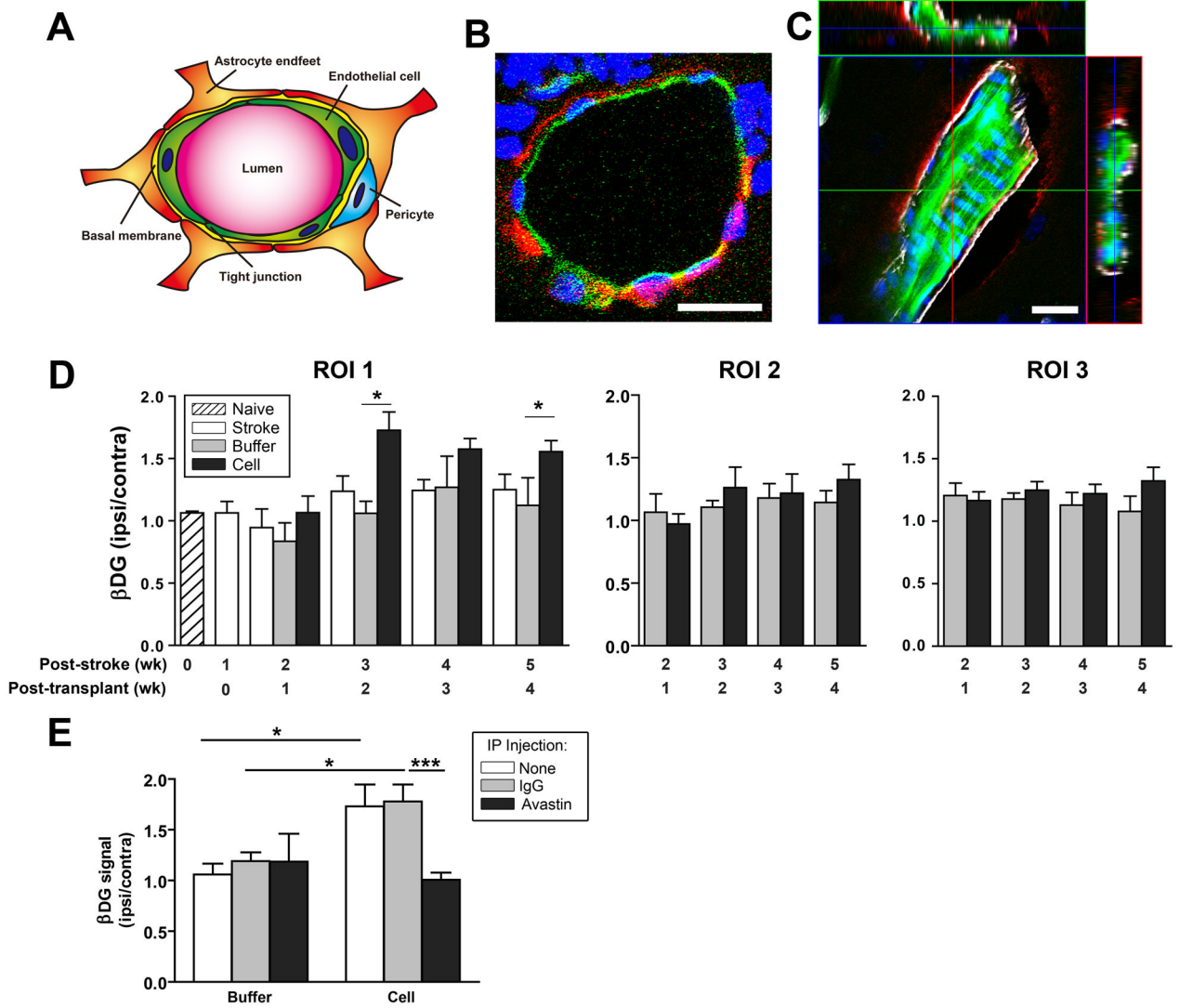


Figure 5. hCNS-SCNs enhance -dystroglycan protein expression after stroke
 (A) Schematic of cellular components of the blood brain barrier. (B) DG (red) does not colocalize with endothelial cells at least in the larger vessels (green, lectin) but does colocalize with the astrocytic end foot marker Aquaporin-4 (white) (C). Scale: 20µm. (D) Quantification of βDG expression in the ROIs over time (defined in Figure 2). hCNS-SCNs significantly enhance βDG levels in the peri-infarct area starting 2 wk post-transplantation; p=0.01 by one way ANOVA at both 2 wk and 4 wk post-transplantation with * p<0.05 by Tukey post-hoc test; N as in Figure 1. (E) Avastin blocks hCNS-SCNs-enhanced βDG expression at 2 wk post-transplantation; * p<0.05; *** p<0.001 by t-test. N=4 for buffer/Avastin, n=5–8 for all other groups.

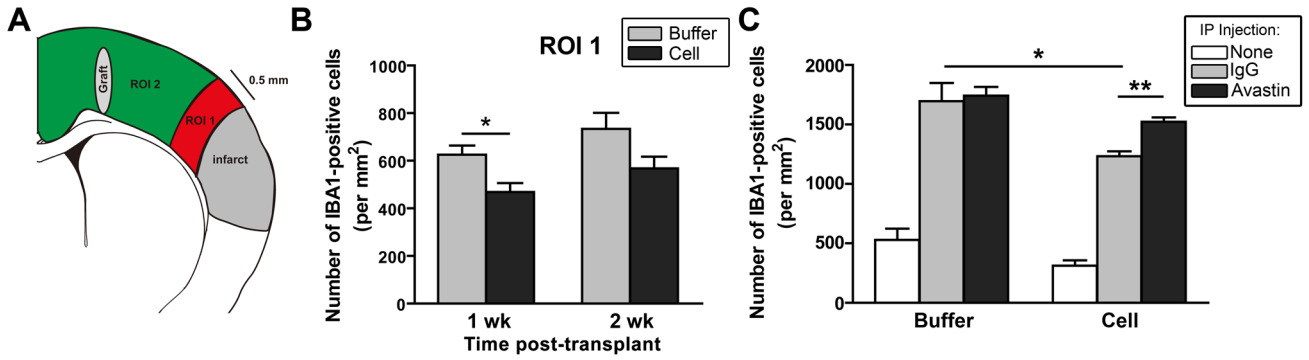


Figure 6. hCNS-SCns reduce inflammation after stroke

(A) Schematic showing ROIs for Iba 1-positive monocytes/macrophages counting. The peri-infarct region (ROI 1) is defined as the area extending 0.5 mm from the lesion edge. (B) Stereological counting revealed that hCNS-SCns-treated animals have fewer Iba 1-positive cells than buffer-treated animals in ROI 1 at 1 wk post-transplantation. * $p < 0.05$ by t-test; $n = 4-6$. (C) In IgG-injected animals, hCNS-SCns still had less inflammation than buffer-treated animals; this immunosuppression was inhibited by Avastin. * $p < 0.05$; ** $p < 0.01$ by t-test; $n = 4$ buffer/Avastin, $n = 5-6$ for all other groups.

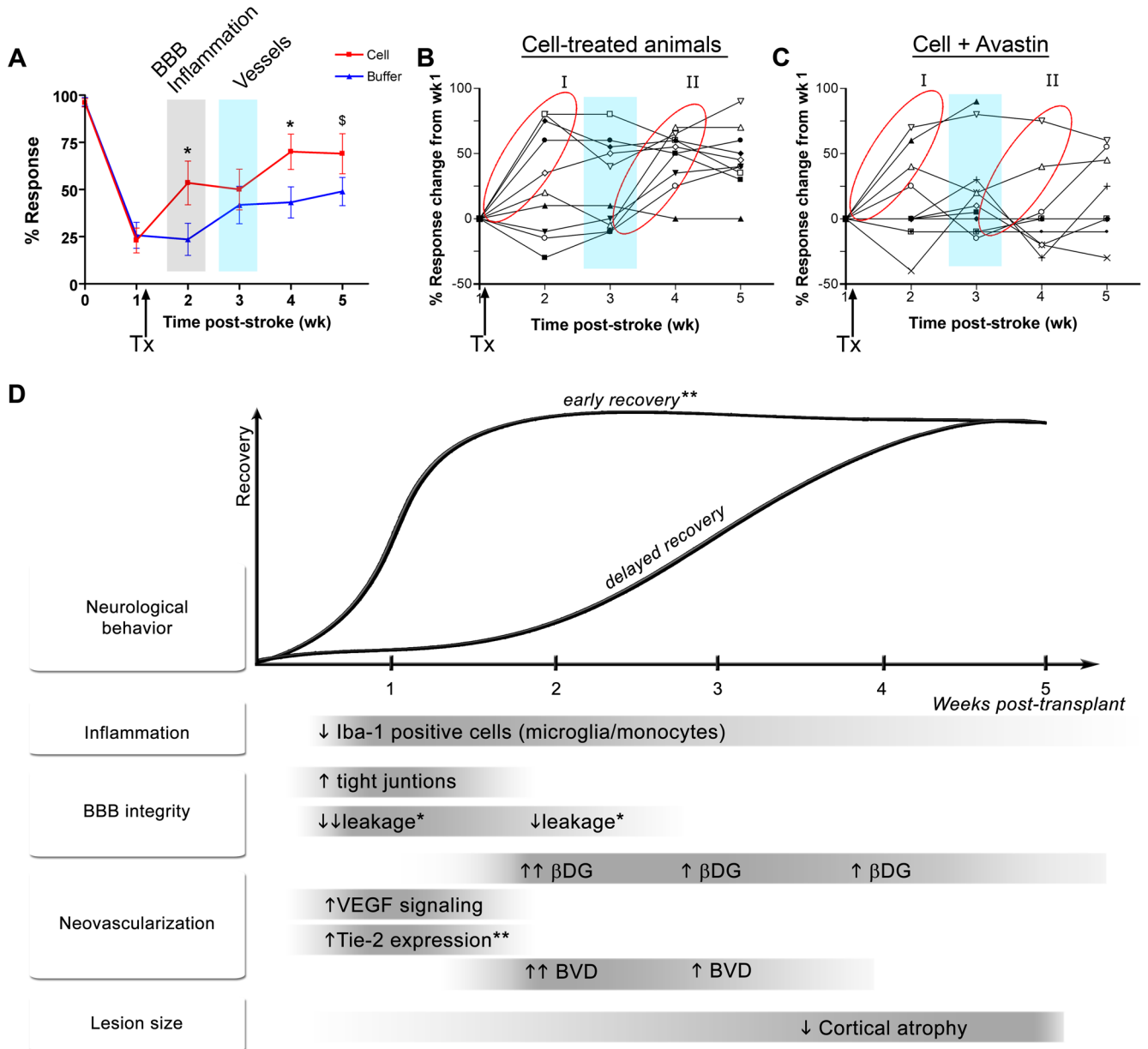


Figure 7. Correlation of hCNS-SCNs-induced recovery with hCNS-SCNs-induced brain changes (A) Overlaying the recovery graph with timing of hCNS-SCNs-induced brain changes reveals that early cell-enhanced recovery occurs before changes in neovascularization. (B) Graph of the behavioral response of individual cell-treated animals reveals two distinct groups of recovery, I and II. (C) Graph of the behavior response of individual cell/Avastin-treated animals; Avastin blocks recovery of Group II. Arrow indicates time of transplantation (TX). Blue vertical bar: time of peak neovascularization. (D) Schematic summarizing the changes induced by transplanted hCNS-SCNs and the temporal relationship of these events to each other and to hCNS-SCNs-enhanced functional recovery. Avastin affected all parameters except for the ones marked *. Inconclusive effects of Avastin are indicated by **.